



OPEN ACCESS

EDITED BY

László Dr. Maródi,
The Rockefeller University,
United States

REVIEWED BY

Oksana Boyarchuk,
Ternopil State Medical University,
Ukraine
Aurélien Guffroy,
Hôpitaux Universitaires de
Strasbourg, France

*CORRESPONDENCE

Marcin Ziętkiewicz
marcin.zietkiewicz@gumed.edu.pl

[†]These authors have contributed
equally to this work

SPECIALTY SECTION

This article was submitted to
Primary Immunodeficiencies,
a section of the journal
Frontiers in Immunology

RECEIVED 29 August 2022

ACCEPTED 11 October 2022

PUBLISHED 25 October 2022

CITATION

Ziętkiewicz M, Buda N,
Więsik-Szewczyk E, Piskunowicz M,
Grzegowska D, Jahnz-Różyk K and
Zdrojewski Z (2022) Comparison of
pulmonary lesions using lung
ultrasound and high-resolution
computed tomography in adult
patients with primary humoral
immunodeficiencies.
Front. Immunol. 13:1031258.
doi: 10.3389/fimmu.2022.1031258

COPYRIGHT

© 2022 Ziętkiewicz, Buda,
Więsik-Szewczyk, Piskunowicz,
Grzegowska, Jahnz-Różyk and
Zdrojewski. This is an open-access
article distributed under the terms of
the [Creative Commons Attribution
License \(CC BY\)](https://creativecommons.org/licenses/by/4.0/). The use, distribution
or reproduction in other forums is
permitted, provided the original author
(s) and the copyright owner(s) are
credited and that the original
publication in this journal is cited, in
accordance with accepted academic
practice. No use, distribution or
reproduction is permitted which does
not comply with these terms.

Comparison of pulmonary lesions using lung ultrasound and high-resolution computed tomography in adult patients with primary humoral immunodeficiencies

Marcin Ziętkiewicz^{1*†}, Natalia Buda^{1†}, Ewa Więsik-Szewczyk²,
Maciej Piskunowicz³, Dominika Grzegowska⁴,
Karina Jahnz-Różyk² and Zbigniew Zdrojewski¹

¹Department of Rheumatology, Clinical Immunology, Geriatrics and Internal Medicine, Medical University of Gdańsk, Gdańsk, Poland, ²Department of Internal Medicine, Pneumology, Allergology and Clinical Immunology, Central Clinical Hospital of the Ministry of National Defense, Military Institute of Medicine, Warsaw, Poland, ³Department of Radiology, Medical University of Gdańsk, Gdańsk, Poland, ⁴Care and Treatment Facility, University Clinical Center, Gdańsk, Poland

Pulmonary involvement is the most common complication in patients with predominantly antibody deficiencies (PADs). Therefore, patients require repeated imaging tests. Unlike high-resolution computed tomography (HRCT), lung ultrasonography (LUS) does not expose patients to X-rays or contrast agents, and can be performed even at the bedside. This study aimed to evaluate lung lesions using simultaneous LUS and HRCT in a group of patients with PADs. Twenty-nine adult patients (13 women and 16 men) diagnosed with PADs according to the ESID criteria (23 Common variable immunodeficiency, 2 X-linked agammaglobulinemia, 2 IgG subclass deficiencies, and 2 Unspecified hypogammaglobulinemia) were included in the study. The mean age was 39.0 ± 11.9 years. The mean time elapsed between the first symptoms of PADs and the examination was 15.4 ± 10.1 years. Lung ultrasonography and high-resolution computed tomography were performed simultaneously according to a defined protocol during the clinic visits. In both examinations, lesions were compared in the same 12 regions: for each lung in the upper, middle, and lower parts, separately, front and back. A total of 435 lesions were described on LUS, whereas 209 lesions were described on HRCT. The frequencies of lesions in the lung regions were similar between LUS and HRCT. In both examinations, lesions in the lower parts of the lungs were most often reported (LUS 60.9% vs. HRCT 55.5%) and least often in the upper parts of the lungs (LUS 12.7% vs. HRCT 12.0%). The most frequently described lesions were LUS consolidations (99; 22.8%) and HRCT fibrosis (74; 16.5%). A statistically significant relationship was found in the detection of fibrosis in 11 of the 12 regions ($\phi = 0.4-1.0$). Maximum values of the ϕ coefficient for the upper part of the left lung were recorded. Compared with

HRCT, LUS is an effective alternative for evaluating and monitoring pulmonary lesions in adult patients with PADs, especially for pulmonary fibrosis.

KEYWORDS

Lung ultrasonography, high-resolution computed tomography, chest sonography, antibody deficiencies, immunodeficiency, pulmonary fibrosis, interstitial lung disease

Introduction

According to the classification developed in 2019, the group of diseases defined as inborn errors of immunity (IEIs) includes over 400 entities (1). However, it should be emphasized that new diseases are described every year. IEIs represent a heterogeneous group of diseases with significantly different clinical presentations. The epidemiology of IEI is challenging to estimate, but in most registries, at least half of the cases are classified as predominantly antibody deficiencies (PADs) (2). Among others, this group includes diseases such as common variable immunodeficiency (CVID), X-linked agammaglobulinemia (XLA), or immunoglobulin G subclass deficiency.

Pulmonary complications are estimated to affect about 60% of patients with PADs and up to 90% patients with CVID (3). Recurrent bacterial respiratory infections are the leading symptoms in this patient group (4) and are often the main reason for the expansion of the diagnosis of primary immunodeficiencies. Frequent or severe respiratory infections can cause structural lung damage that may promote chronic pulmonary diseases such as bronchiectasis, atelectasis, or fibrosis. Early diagnosis and management with prophylactic antibiotics and Ig replacement therapy reduce the frequency of infections and their long-term effects (5).

Many patients with PAD also have pulmonary non-infectious complications such as the previously mentioned bronchiectasis or fibrosis, as well as asthma, interstitial disease, or malignancy. Depending on the population studied, the incidence of complications is various. It is estimated that asthma occurs in 31.2% of patients with CVID and 10.3% of patients with XLA (6). Bronchiectasis occurs in 25 to 79% of patients with PADs (7–9). Less common is interstitial lung disease (ILD), described mainly in patients with CVID (10–20%) (8). A particular form of ILD is granulomatous-lymphocytic interstitial lung disease (GLILD), which is described mainly in the course of CVID with a frequency of about 8–20% (10). The rarest non-infectious complication is malignancy. The most common are lymphomas, the incidence of which is estimated at less than 10% of patients (9).

Pulmonary complications in patients with PADs not only impair their quality of life, but also contribute to higher mortality. In patients with CVID, it has been estimated that

the risk of death increases twofold if there are functional or structural changes in the lungs (11). A higher incidence of extrapulmonary complications such as splenomegaly, lymphomas, autoimmunity (especially autoimmune cytopenias), has been described among patients with GLILD (10).

Lung imaging studies should be performed to detect pulmonary complications of PADs. Such examinations are sometimes repeated multiple times during a patient's lifetime to monitor the disease. Currently, the gold standard for diagnosis is computed tomography (CT), especially high-resolution computed tomography (HRCT) (7, 12). Performing these tests is associated with patient exposure to X-rays or contrast agents. This limits their ability to perform tasks frequently. It is worth noting that increased radiosensitivity has also been demonstrated in patients with CVID compared with healthy individuals (13).

Lung ultrasonography (LUS) does not have these disadvantages. This method allows non-invasive diagnosis of the pleural cavities, pleura, and lungs. A disadvantage of LUS, and a prerequisite for imaging pulmonary lesions, is that they are in direct contact with the pleural line. It is essential that the examination is performed at the patient's bedside. This could be helpful when pulmonary imaging monitoring is necessary. The patient does not require any preparation, and the procedure can be repeated many times, even at short intervals.

Ultrasonography of the lungs has been an underestimated diagnostic method for many years. An appropriate air lung is a barrier to the propagation of ultrasonic waves. Initially, ultrasound was used for years only for the diagnosis of pathological lesions in the pleural cavity (fluid, neoplastic lesions of the chest wall) (14). As a result of lung disease, there is a loss of aeration (total or partial), and lesions appear on ultrasound, which are referred to as artifacts or consolidations. The artifacts do not correspond to anatomical structures but are formed when lung aeration is reduced (15). Artifacts are often accompanied by pleural lines (on the lung surface) and subpleural lesions. The constellation of individual artifacts, pleural lines, and subpleural lesions facilitates the differentiation of infectious interstitial lesions, cardiogenic pulmonary edema, and pulmonary fibrosis. The second type of lesion is a consolidation, that is, area of airless lung. Other ultrasound symptoms coexist with consolidations, allowing for

further differential diagnosis of inflammatory changes such as atelectasis, infarction in the course of pulmonary embolism, and metastatic changes or abscesses (16).

The last few decades have seen an increase in the number of original publications that show promise for the use of ultrasonography in the imaging diagnosis of pulmonary lesions. To date, well-developed criteria include lesions in which there is consolidation of the pulmonary parenchyma (pneumonia, atelectasis, lesions in the course of pulmonary embolism) and interstitial lesions (cardiogenic pulmonary edema, interstitial pneumonia, pulmonary fibrosis in the course of interstitial lung disease) (17–20). The results of numerous studies make it possible to consider LUS as a useful method for the diagnosis of lung lesions in examinations using X-rays (19, 20). Lung US is particularly well-established for lower respiratory tract infections in children (21, 22).

Despite numerous possible pulmonary complications in the course of IEI, we did not find data on the ultrasound images of the lungs in this group of patients in the available literature. The aim of our study was to characterize the lesions in the lungs that can be visualized using LUS in a group of patients with PADs. An additional goal was to compare the lung images obtained using ultrasound with those obtained using high-resolution tomography.

Material and methods

Study group

Twenty-nine patients (13 women and 16 men) with PADs (23 with COVID, 2 with XLA, 2 with IgG subclass deficiencies, and 2 with unspecified hypogammaglobulinemia) were included in this study. The mean age at the onset of the first symptoms was 23.6 ± 13.6 years. The mean diagnosis delay was 8.0 ± 9.0 years. At the time of testing, the mean age, was 39.0 ± 11.9 years. The mean time between the first symptoms of PADs and the examination was 15.4 ± 10.1 years. All patients received immunoglobulin replacement therapy (3 IVIG and 26 SCIG/fSCIG). The mean IgG concentration at the time of lung imaging studies was 8.4 ± 1.8 g/l. Most patients (26/29, 89.7%) declared that they had a history of recurrent lower respiratory tract infections. Twelve patients had infections only until the diagnosis of PADs was made and immunoglobulin replacement therapy introduced. While imaging studies were performed, we did not observe any clinical signs of respiratory tract infections. The most common noninfectious complication was polyclonal lymphoproliferation ($n=16$; 55.2%), followed by 51.7% autoimmunity, 44.8% pulmonary fibrosis, 34.5% bronchiectasis, 17.2% GLLD and 13.8% asthma. A detailed characteristic of the population is available in the [Supplementary Material](#).

The inclusion criteria were as follows: age ≥ 18 years, diagnosis of PADs according to the diagnostic criteria of the

European Society for Immunodeficiencies (23), and provision of written consent. The exclusion criteria were as follows: unfulfilled inclusion criteria, symptoms of acute respiratory tract infection, and in the case of women, pregnancy.

Lung ultrasound

Lung ultrasound was performed with a PHILIPS ultrasound scanner (year of manufacture 2016, WA, USA) using two probes: convex (2–6 MHz) and linear (4–12 MHz). Ultrasound examination of the lungs was performed according to a protocol involving scanning the entire lung surface available during the ultrasound examination bilaterally over the posterior, lateral, and anterior chest wall. We presented an ultrasound image of a normal lung in [Figure 1](#).

The lesions observed in each lung field were anonymized in a dedicated form and submitted for statistical analysis. Ultrasound examinations were performed by a lung ultrasound specialist with 12 years of experience. Pulmonary fibrosis was assumed to be present in a region if the following criteria were met: pleural lesions (irregularity, fragmentation, blurred pleural line), vertical artifacts (B lines, Z lines, C lines), and subpleural consolidations. In [Figure 2](#), we have shown examples of pathological changes in lung ultrasound images.

Chest high-resolution tomography

Chest HRCT scans were obtained using a 128-detector row Siemens Somatom Flash scanner (Siemens, Forchheim, Germany). Images were obtained in the craniocaudal direction during a single breath-hold with collimation 128×0.6 mm, rotation time 0.5 s, matrix 512×512 mm, and 0.6 mm reconstructed section thickness. Image analysis was performed using dedicated software (Syngo.via, Siemens) and an application (CT Chest in Syngo.via) with standard lung window settings (width, -50 HU; level, 1500 HU) and mediastinal window settings (width, 350 HU; level, 50 HU). HRCT was performed within 2 hours of lung ultrasound.

The lesions observed on HRCT were described in detail in a form dedicated to CT lesion descriptions and anonymized for further statistical analysis. Computed tomographic scans were reviewed by a radiologist with 18 years of experience. In both examinations, lesions were compared in the same 12 regions: for each lung in the upper, middle, and lower parts, separately, front and back.

Statistical methods

Statistical analyses were performed using the STATISTICA software (version 13; TIBCO Software Inc., Palo Alto, CA, USA). To determine the relationship between abnormalities detected

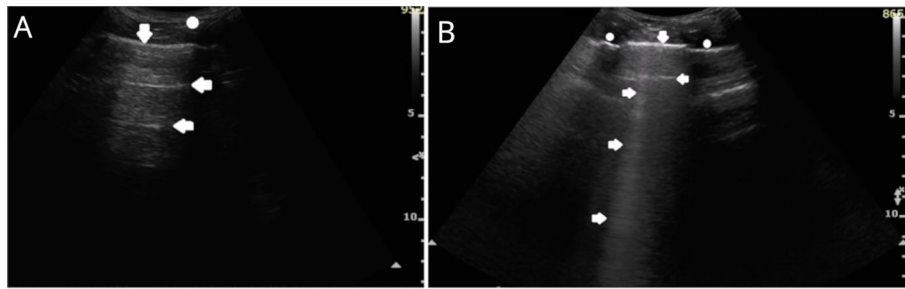


FIGURE 1
Image of normal lung on ultrasonography. **(A)** structures of chest wall (o), smooth and regular pleural line (↓), A lines, horizontal artifacts observed in properly aerated lung (←). Convex probe (1-6MHz). **(B)** ribs and anechoic shadow behind them (o), smooth and regular pleural line (↓), A line artifact (←), B line, vertical artifact of comet tail, in some objects visible in the last intercostal space as a normal variant (→). Convex probe (1-6MHz).

on HRCT and LUS, a chi-square test or Fisher’s exact test (when the expected number was smaller than five) was employed with the phi coefficient as a measure of the power of correlation. Statistical significance was assumed at $p < 0.05$.

Gdansk, Gdańsk, Poland. All participants provided written informed consent to participate in the study.

Results

Bioethics committee

Studies involving human participants were reviewed and approved by the Ethics Committee of the Medical University of

Lung ultrasonography

We described 435 lesions on lung ultrasonography in our study group of 29 patients with predominantly antibody

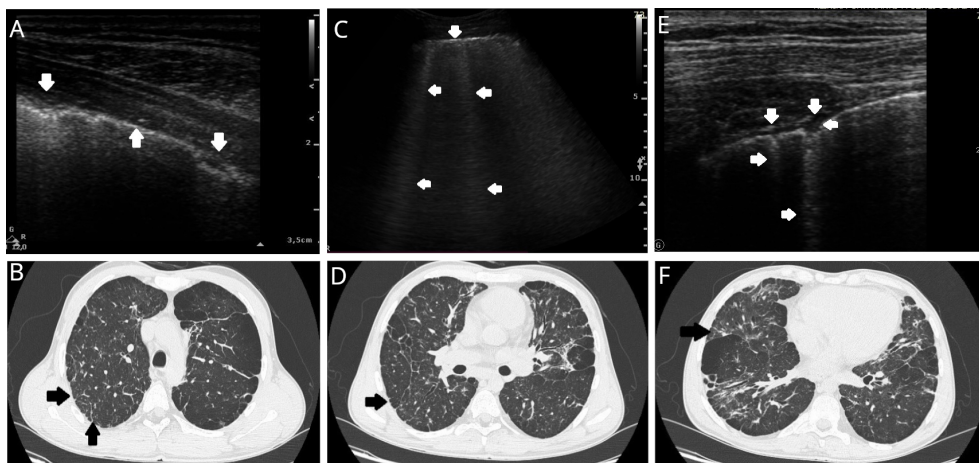


FIGURE 2
Examples of lung lesions in a patient with predominantly antibody deficiency on lung ultrasound (LUS) and high-resolution tomography (HRCT). **(A)** LUS: Irregular and infiltrated pleural line (↓), regular pleural line (↑). Linear probe. **(B)** HRCT (axial plane): Right lung - peripheral paraseptal emphysema with centrilobular emphysema inside the lung and fibrosis, thickening of the pleura between the arrows with subpleural fibrosis (arrowheads). Left lung combined centrilobular and panlobular emphysema with fibrosis. **(C)** LUS: Irregular pleural line (↓) and multiple B lines (←). Convex probe (1-6MHz). **(D)** HRCT (axial plane): Right lung - peripheral paraseptal emphysema with centrilobular emphysema inside the lung and fibrosis (arrowhead). Left lung combined paraseptal and centrilobular emphysema with fibrosis. **(E)** LUS: Irregular pleural line, and small subpleural consolidation (↓←) with vertical artifact C line (arising from subpleural lesion) (→). Linear probe. **(F)** HRCT (axial plane): Right lung - combined paraseptal, centrilobular and panlobular emphysema and fibrosis, thickening of the pleura with subpleural fibrosis (arrowhead). Left lung combined paraseptal, centrilobular and panlobular emphysema with fibrosis.

deficiency. Most lesions were located in the lower regions of the lungs (265; 60.9%). The numbers of lesions in the middle and upper parts were 115 (26.4%) and 55 (12.7%), respectively. The most frequently described lesion was consolidation (n = 99; 22.8%). The frequencies of other lesions were as follows: C-lines (94, 21.6%), irregular pleural lines (93, 21.4%), B-lines (57, 13.1%), fragmented pleural line (45, 10.3%), blurred pleural lines (24, 5.5%), and Z-lines (23, 5.3%). **Table 1** shows the number of lesions described in each of the 12 lung regions examined in this study. Pulmonary fibrosis, diagnosed according to the established definition, was diagnosed 79 times. Fibrosis was most common in the lower lung (48; 60.8%). In the middle and upper regions of the lungs, 20 (25.3%) and 11 (13.9%) lesions were suggestive of fibrosis, respectively (**Table 2**). In five patients (17.2%), no pathological lesions were detected on ultrasound.

High-sensitive computed tomography

Compared with LUS, the number of lesions described on HRCT was lower, amounting to 209. However, in this study, we also described most changes in the lower parts of the lungs (116; 55.5%). There were 25 (12.0%) and 68 (32.5%) lesions in the upper and middle lung regions, respectively (**Table 1**). The most frequently described lesion was fibrosis (n = 74, 16.5%). The frequencies of other lesions were as follows: tree-in-bud pattern (27, 6.0%), pleural thickening (23, 5.1%), pleural adhesions (23, 5.1%), bronchiectasis (22, 4.9%), thickening of the intertrabecular septum (16, 3.6%), emphysema bulls (9, 2%), consolidations < 5 mm (8, 1.8%), and calcifications (7, 1.6%). In three patients (10.3%), no pathological changes were observed on HRCT. Examples of pathological changes observed on HRCT are shown in **Figure 2**.

TABLE 1 Distribution of each lesion detected in lung ultrasound (LUS) and high-resolution computed tomography (HRCT) by lung region.

Lesions	LUNG ULTRASONOGRAPHY				Lesions	HIGH-RESOLUTION COMPUTED TOMOGRAPHY			
	FRONT		BACK			FRONT		BACK	
	LEFT	RIGHT	LEFT	RIGHT		LEFT	RIGHT	LEFT	RIGHT
TOP					Fibrosis	1 (3.4%)	5 (17.2%)	2 (6.9%)	5 (17.2%)
Blurred PL	1 (3.4%)	0 (0.0%)	0 (0.0%)	0 (0.0%)	PL thickening	0 (0.0%)	0 (0.0%)	2 (6.9%)	1 (3.4%)
Irregular PL	2 (6.9%)	1 (3.4%)	2 (6.9%)	4 (13.8%)	Calcifications	0 (0.0%)	0 (0.0%)	1 (3.4%)	0 (0.0%)
Fragmented PL	1 (3.4%)	0 (0.0%)	0 (0.0%)	3 (10.3%)	PL adhesions and clusters	0 (0.0%)	0 (0.0%)	0 (0.0%)	1 (3.4%)
B-lines	2 (6.9%)	3 (10.3%)	3 (10.3%)	0 (0.0%)	Bronchiectasis	0 (0.0%)	0 (0.0%)	0 (0.0%)	1 (3.4%)
C-lines	4 (13.8%)	4 (13.8%)	2 (6.9%)	4 (13.8%)	Emphysema bulls	0 (0.0%)	1 (3.4%)	0 (0.0%)	1 (3.4%)
Z-lines	1 (3.4%)	2 (6.9%)	1 (3.4%)	1 (3.4%)	Thickening of the ILS	0 (0.0%)	0 (0.0%)	1 (3.4%)	1 (3.4%)
Consolidations	4 (13.8%)	4 (13.8%)	2 (6.9%)	4 (13.8%)	Consolidations	0 (0.0%)	0 (0.0%)	0 (0.0%)	0 (0.0%)
					Tree-in-bud	0 (0.0%)	1 (3.4%)	0 (0.0%)	1 (3.4%)
MIDDLE					Fibrosis	4 (13.8%)	6 (20.7%)	5 (17.2%)	8 (27.6%)
Blurred PL	1 (3.4%)	1 (3.4%)	0 (0.0%)	1 (3.4%)	PL thickening	1 (3.4%)	0 (0.0%)	5 (17.2%)	5 (17.2%)
Irregular PL	5 (17.2%)	7 (24.1%)	6 (20.7%)	6 (20.7%)	Calcifications	0 (0.0%)	0 (0.0%)	1 (3.4%)	1 (3.4%)
Fragmented PL	3 (10.3%)	4 (13.8%)	3 (10.3%)	3 (10.3%)	PL adhesions and clusters	2 (6.9%)	0 (0.0%)	0 (0.0%)	0 (0.0%)
B-lines	2 (6.9%)	2 (6.9%)	5 (17.2%)	6 (20.7%)	Bronchiectasis	1 (3.4%)	2 (6.9%)	1 (3.4%)	2 (6.9%)
C-lines	9 (31.0%)	10 (34.5%)	2 (6.9%)	5 (17.2%)	Emphysema bulls	1 (3.4%)	0 (0.0%)	1 (3.4%)	1 (3.4%)
Z-lines	1 (3.4%)	3 (10.3%)	2 (6.9%)	1 (3.4%)	Thickening of the ILS	1 (3.4%)	3 (10.3%)	1 (3.4%)	2 (6.9%)
Consolidations	9 (31.0%)	10 (34.5%)	3 (10.3%)	5 (17.2%)	Consolidations	0 (0.0%)	1 (3.4%)	0 (0.0%)	3 (10.3%)
					Tree-in-bud	1 (3.4%)	2 (6.9%)	3 (10.3%)	4 (13.8%)
BOTTOM					Fibrosis	8 (27.6%)	9 (31.0%)	13 (44.8%)	8 (27.6%)
Blurred PL	6 (20.7%)	5 (17.2%)	5 (17.2%)	4 (13.8%)	PL thickening	0 (0.0%)	1 (3.4%)	4 (13.8%)	4 (13.8%)
Irregular PL	15 (51.7%)	15 (51.7%)	14 (48.3%)	16 (55.2%)	Calcifications	1 (3.4%)	2 (6.9%)	0 (0.0%)	1 (3.4%)
Fragmented PL	6 (20.7%)	8 (27.6%)	8 (27.6%)	6 (20.7%)	PL adhesions and clusters	7 (24.1%)	5 (17.2%)	5 (17.2%)	3 (10.3%)
B-lines	5 (17.2%)	9 (31.0%)	11 (37.9%)	9 (31.0%)	Bronchiectasis	3 (10.3%)	4 (13.8%)	6 (20.7%)	2 (6.9%)
C-lines	15 (51.7%)	16 (55.2%)	10 (34.5%)	13 (44.8%)	Emphysema bulls	1 (3.4%)	1 (3.4%)	1 (3.4%)	1 (3.4%)
Z-lines	5 (17.2%)	4 (13.8%)	0 (0.0%)	2 (6.9%)	Thickening of the ILS	1 (3.4%)	2 (6.9%)	3 (10.3%)	1 (3.4%)
Consolidations	15 (51.7%)	16 (55.2%)	14 (48.3%)	13 (44.8%)	Consolidations	3 (10.3%)	1 (3.4%)	0 (0.0%)	0 (0.0%)
					Tree-in-bud	3 (10.3%)	4 (13.8%)	5 (17.2%)	3 (10.3%)

PL, pleural line; ILS, interlobular septum.

Frequency is shown using a color scale from lowest (green) to highest (red) separately for LUS and HRCT.

TABLE 2 Analysis of the frequency of fibrosis with the coefficient phi for the correlations between findings detected in lung ultrasound and high-resolution computed tomography.

TOP	USG	FRONT								BACK										
		LEFT				RIGHT				LEFT				RIGHT						
		HRCT		USG	HRCT		USG	HRCT		USG	HRCT		USG	HRCT						
No	Yes	No	Yes		No	Yes		No	Yes		No	Yes								
		N	%	N	%			N	%	N	%			N	%	N	%			
	No	26	100.0 %	0	0.0 %	No	24	100.0 %	1	20.0 %	No	27	100.0 %	0	0.0 %	No	24	100.0 %	3	60.0 %
	Yes	0	0.0 %	3	100.0 %	Yes	0	0.0 %	4	80.0 %	Yes	0	0.0 %	2	100.0 %	Yes	0	0.0 %	2	40.0 %
		p	<0.001	Phi	1.00		p	<0.001	Phi	0.876		p	0.002	Phi	1.00		p	0.025	Phi	0.596
MIDDLE	USG	FRONT								BACK										
		LEFT				RIGHT				LEFT				RIGHT						
		HRCT		USG	HRCT		USG	HRCT		USG	HRCT		USG	HRCT						
No	Yes	No	Yes		No	Yes		No	Yes		No	Yes								
		N	%	N	%			N	%	N	%			N	%	N	%			
	No	22	100.0 %	4	57.1 %	No	22	95.7 %	0	0.0 %	No	22	100.0 %	2	28.6 %	No	17	94.4 %	7	63.6 %
	Yes	0	0.0 %	3	42.9 %	Yes	1	4.3 %	6	100.0 %	Yes	0	0.0 %	5	71.4 %	Yes	1	5.6 %	4	36.4 %
		p	0.010	Phi	0.602		p	<0.001	Phi	0.905		p	<0.001	Phi	0.809		p	0.054	Phi	0.396
BOTTOM	USG	FRONT								BACK										
		LEFT				RIGHT				LEFT				RIGHT						
		HRCT		USG	HRCT		USG	HRCT		USG	HRCT		USG	HRCT						
No	Yes	No	Yes		No	Yes		No	Yes		No	Yes								
		N	%	N	%			N	%	N	%			N	%	N	%			
	No	13	86.7 %	6	42.9 %	No	11	78.6 %	4	26.7 %	No	10	83.3 %	6	35.3 %	No	13	86.7 %	5	35.7 %
	Yes	2	13.3 %	8	57.1 %	Yes	3	21.4 %	11	73.3 %	Yes	2	16.7 %	11	64.7 %	Yes	2	13.3 %	9	64.3 %
		p	0.021	Phi	0.461		p	0.009	Phi	0.519		p	0.022	Phi	0.476		p	0.008	Phi	0.525

Comparison of pulmonary fibrosis in HRCT and LUS

We found no correlation between the occurrence of individual lesions on LUS and lesions observed on HRCT. However, it should be emphasized that the analysis of LUS results is based on the occurrence of certain combinations of symptoms rather than individual findings.

To compare the diagnostic capabilities of HRCT and LUS, we assessed the incidence of lesions indicative of pulmonary fibrosis in both studies. We chose fibrosis because it is the most frequently described lesion on computed tomography, and a set of ultrasound signs are known to identify this process in LUS. Table 2 summarizes the prevalence of fibrosis in the 12 examined regions of the lungs. A statistically significant relationship between the results of both imaging studies was found in 11 regions. The strength of the relationship was strong (phi = 0.40–0.69) or very strong (phi ≥ 0.70). The maximum values of the phi coefficient for the upper part of the left lung were recorded (phi = 1.0). Only the result for the back in the middle of the right lung was at the limit of statistical significance (p = 0.054). In the same region, the strength of the association between the results of the two examinations, assessed using the phi coefficient, was the weakest (phi = 0.396).

Discussion

Lung disease is a frequent complication of PADs with high morbidity and mortality rates. The spectrum of clinical

manifestations is broad, and includes acute and chronic infections, structural abnormalities, and malignancies (3, 8). All these disorders have in common that diagnostic imaging is necessary to establish the diagnosis and monitor progression. Currently, we mainly use computed tomography for this purpose (7). In many groups of patients, the usefulness of lung ultrasound, which has been developing intensely in recent years, has been proven. To our knowledge, ultrasound lung lesions in patients with primary immunodeficiencies have not yet been described.

In our group of 29 patients with PADs, the lesions described on both LUS and HRCT were usually diffuse rather than focal. In most cases, the lesions closely resembled those described in interstitial lung disease. Twenty-four patients had multiple ultrasound abnormalities in the form of artifacts (B-, C-, and Z-line artifacts), pleural line lesions (irregular, fragmented, and blurred), and small subpleural consolidations (< 5 mm). Consolidations and accompanying pleural line lesions in the LUS were the most frequent, which may indicate lesions in the interstitial space and alveoli. These lesions may be secondary to atelectasis or post-inflammatory changes, which may be due to previous recurrent lower respiratory tract infections. It should be noted that vertical artifacts observed in large numbers upon LUS examination are an indirect parameter indicating a problem located in the interstitial space of the lungs or in the subpleural area.

The higher number of pleural lesions described on lung ultrasound than on HRCT may be due to technical differences

between these examinations. LUS allows for very accurate imaging of the pleural line and superficial parts of the lungs compared to CT. If interstitial lung lesions are predominant, LUS does not allow the assessment of deeper lung areas. On the other hand, computed tomography allows deep evaluation of the lung up to the mediastinum. Lung ultrasound and HRCT are complementary and used together may allow for improved diagnostic and monitoring capabilities for patients with PADs.

In our group, both LUS and HRCT showed that the lesions accumulated mainly in the lower and middle parts of the lungs. These observations are consistent with previously published lesion locations on HRCT in patients with PADs. Both Tanaka et al. (24) and Bondionii et al. (25) observed very few lesions in adult patients with COVID and XLA in the upper lung on HRCT. They were predominantly in the middle and lower parts. However, the accumulation of lesions in the lower lobes of the lungs, as observed in our study, has not been described.

In the CT scan performed up to 2 h after the LUS, numerous non-specific abnormalities were found in the studied patients. We found no correlation between individual lesions on LUS examination and lesions observed on HRCT. This is due to the fact that in LUS, it is not individual lesions but their co-occurrence in certain constellations that should be evaluated. This makes it impossible to directly compare the deviations described by the lung imaging techniques.

The most common lesions on HRCT are indicative of lung fibrosis. In case of LUS, we defined the features of the ultrasound image that indicated the presence of this pathology. We demonstrated a statistically significant and strong correlation between fibrotic images on LUS and HRCT. This supports the usefulness of ultrasonography in the diagnosis of pulmonary fibrosis, which is also described for idiopathic pulmonary fibrosis (26) or lesions in the course of systemic connective tissue diseases (19).

In the study group, no patient was found to have neoplastic disease; therefore, it is not possible to conclude on the diagnostic possibilities of neoplastic disease with lung ultrasonography.

Surprisingly, there were a low number of bronchiectasis cases in the study group. These lesions accounted for approximately 5% of all lesions described on HRCT. Bronchiectasis is a common complication of COVID. In the study group of patients with PADs, the majority had this immunodeficiency. According to various estimates, the percentage of patients with COVID diagnosed with bronchiectasis ranges from 25 to 79% (7). The low incidence of this complication in our group may have been due to well-managed immunoglobulin supplementation. Indeed, a close relationship between the incidence of bronchiectasis and IgG levels has been previously demonstrated (27).

Our study has a few limitations. We included a small group of patients; however, this population was well clinically characterized. This was a pilot study, and we performed the

examinations only once. We did not analyze how the lung lesions changed during a longer follow-up period. Owing to the very high variability of the described abnormalities in both imaging studies and the different clinical presentations of PADs, it is necessary to conduct studies on a larger number of patients. To compare the usefulness of LUS and HRCT, it would be worthwhile to conduct a study on a group of patients with well-defined pulmonary complications. This will allow for a comparison of the two imaging studies in specific clinical situations. In future studies it would be worthwhile to correlate functional test results with lung ultrasound images.

Conclusions

In the study group of patients with predominantly antibody deficiencies, the diagnostic potential of ultrasonography for the evaluation of pulmonary lesions was evaluated. The lesions on LUS and HRCT were non-specific. The features of fibrosis found by both diagnostic methods correlated very well. Lung ultrasonography appears to be a promising method for imaging pulmonary lesions, especially fibrosis, in patients with primary immunodeficiencies. For lesions of a different nature, it is necessary to perform studies on a larger group of patients with strictly defined pulmonary complications.

Data availability statement

The raw data supporting the conclusions of this article will be made available by the authors, without undue reservation.

Ethics statement

The studies involving human participants were reviewed and approved by Ethics Committee of the Medical University of Gdansk, Gdańsk, Poland. The patients/participants provided their written informed consent to participate in this study.

Author contributions

MZ and NB designed the study and wrote the first draft of the manuscript. This text was produced with equal contributions from both authors. MZ, NB, EW-S, and DG collected the data and performed the literature searches. NB performed the lung ultrasound examinations. MP described HRCT findings. MZ performed the statistical analyses. EW-S, ZZ, and KJ-R critically revised the manuscript for intellectual content. All the authors have read and agreed to the published version of the manuscript.

Conflict of interest

The authors declare that the research was conducted in the absence of any commercial or financial relationships that could be construed as potential conflicts of interest.

Publisher's note

All claims expressed in this article are solely those of the authors and do not necessarily represent those of their affiliated

organizations, or those of the publisher, the editors and the reviewers. Any product that may be evaluated in this article, or claim that may be made by its manufacturer, is not guaranteed or endorsed by the publisher.

Supplementary material

The Supplementary Material for this article can be found online at: <https://www.frontiersin.org/articles/10.3389/fimmu.2022.1031258/full#supplementary-material>

References

- Bousfiha A, Jeddane L, Picard C, Al-Herz W, Ailal F, Chatila T, et al. Human inborn errors of immunity: 2019 update of the IUIS phenotypical classification. *J Clin Immunol* (2020) 40:66–81. doi: 10.1007/s10875-020-00758-x
- Abolhassani H, Azizi G, Sharifi L, Yazdani R, Mohsenzadegan M, Delavari S, et al. Global systematic review of primary immunodeficiency registries. *Expert Rev Clin Immunol* (2020) 16:717–32. doi: 10.1080/1744666X.2020.1801422
- Cinetto F, Scarpa R, Rattazzi M, Agostini C. The broad spectrum of lung diseases in primary antibody deficiencies. *Eur Respir Rev* (2018) 27. doi: 10.1183/16000617.0019-2018
- Demirdag YY, Gupta S. Update on infections in primary antibody deficiencies. *Front Immunol* (2021) 12:634181/BIBTEX. doi: 10.3389/FIMMU.2021.634181/BIBTEX
- Busse PJ, Razvi S, Cunningham-Rundles C. Efficacy of intravenous immunoglobulin in the prevention of pneumonia in patients with common variable immunodeficiency. *J Allergy Clin Immunol* (2002) 109:1001–4. doi: 10.1067/mai.2002.124999
- Weinberger T, Fuleihan R, Cunningham-Rundles C, Maglione PJ. Factors beyond lack of antibody govern pulmonary complications in primary antibody deficiency. *J Clin Immunol* (2019) 39:440. doi: 10.1007/S10875-019-00640-5
- Rodríguez JA, Bang TJ, Restrepo CS, Green DB, Browne LP, Vargas D. Imaging features of primary immunodeficiency disorders. *Radiol Cardiothorac Imaging* (2021) 3. doi: 10.1148/RYCT.2021200418
- Casal A, Riveiro V, Suárez-Antelo J, Ferreiro L, Rodríguez-Núñez N, Lama A, et al. Pulmonary manifestations of primary humoral deficiencies. *Can Respir J* (2022) 2022:9. doi: 10.1155/2022/7140919
- Movahedi M, Jamee M, Ghaffaripour H, Noori F, Ghaini M, Eskandarzadeh S, et al. Pulmonary manifestations in a cohort of patients with inborn errors of immunity: an 8-year follow-up study. *Allergol Immunopathol (Madr)* (2022) 50:80–4. doi: 10.15586/AELV5011.388
- Cinetto F, Scarpa R, Carrabba M, Firinu D, Lougaris V, Buso H, et al. Granulomatous lymphocytic interstitial lung disease (GLILD) in common variable immunodeficiency (CVID): A multicenter retrospective study of patients from Italian PID referral centers. *Front Immunol* (2021) 12:627423/BIBTEX. doi: 10.3389/FIMMU.2021.627423/BIBTEX
- Resnick ES, Moshier EL, Godbold JH, Cunningham-Rundles C. Morbidity and mortality in common variable immune deficiency over 4 decades. *Blood* (2012) 119:1650–7. doi: 10.1182/BLOOD-2011-09-377945
- Meerburg JJ, Hartmann IJC, Goldacker S, Baumann U, Uhlmann A, Andrinopoulou ER, et al. Analysis of granulomatous lymphocytic interstitial lung disease using two scoring systems for computed tomography scans—a retrospective cohort study. *Front Immunol* (2020) 11:589148/FULL. doi: 10.3389/FIMMU.2020.589148/FULL
- Mahmoodi M, Abolhassani H, Mozdarani H, Rezaei N, Azizi G, Yazdani R, et al. In vitro chromosomal radiosensitivity in patients with common variable immunodeficiency. *Cent Eur J Immunol* (2018) 43:155. doi: 10.5114/CEJI.2018.77385
- Mayo PH, Copetti R, Feller-Kopman D, Mathis G, Maury E, Mongodi S, et al. Thoracic ultrasonography: a narrative review. *Intensive Care Med* (2019) 45:1200–11. doi: 10.1007/S00134-019-05725-8/TABLES/2
- Mongodi S, de Luca D, Colombo A, Stella A, Santangelo E, Corradi F, et al. Quantitative lung ultrasound: Technical aspects and clinical applications. *Anesthesiology* (2021) 134:949–65. doi: 10.1097/ALN.0000000000003757
- Buda N, Kosiak W, Radzikowska E, Olszewski R, Jassem E, Grabczak EM, et al. Polish recommendations for lung ultrasound in internal medicine (POLLUS-IM). *J Ultrason* (2018) 18:198–206. doi: 10.15557/JOU.2018.0030
- Buda N, Kosiak W, Welnicki M, Skoczylas A, Olszewski R, Piotrkowski J, et al. Recommendations for lung ultrasound in internal medicine. *Diagnostics* (2020) 10:597. doi: 10.3390/diagnostics10080597
- Volpicelli G, Elbarbary M, Blaivas M, Lichtenstein DA, Mathis G, Kirkpatrick AW, et al. International evidence-based recommendations for point-of-care lung ultrasound. *Intensive Care Med* (2012) 38:577–91. doi: 10.1007/S00134-012-2513-4/FIGURES/2
- Buda N, Wojteczek A, Masiak A, Piskunowicz M, Batko W, Zdrojewski Z. Lung ultrasound in the screening of pulmonary interstitial involvement secondary to systemic connective tissue disease: A prospective pilot study involving 180 patients. *J Clin Med* (2021) 10:4114. doi: 10.3390/jcm10184114
- Rodríguez-Contreras FJ, Calvo-Cebrián A, Díaz-Lázaro J, Cruz-Arnés M, León-Vázquez F, del Carmen Lobón-Agúndez M, et al. Lung ultrasound performed by primary care physicians for clinically suspected community-acquired pneumonia: A multicenter prospective study. *Ann Fam Med* (2022) 20:227–36. doi: 10.1370/AFM.2796
- Jaworska J, Komorowska-Piotrowska A, Pomiećko A, Wiśniewski J, Woźniak M, Littwin B, et al. Consensus on the application of lung ultrasound in pneumonia and bronchiolitis in children. *Diagnostics* (2020) 10:935. doi: 10.3390/DIAGNOSTICS10110935
- Dietrich CF, Buda N, Ciuca IM, Dong Y, Fang C, Feldkamp A, et al. Lung ultrasound in children, WFUMB review paper (part 2). *Med Ultrason* (2021) 23:443–52. doi: 10.11152/MU-3059
- ESID - European Society for Immunodeficiencies. Available at: <https://esid.org/Working-Parties/Registry-Working-Party/Diagnosis-criteria> (Accessed August 27, 2022).
- Tanaka N, Kim JS, Bates CA, Brown KK, Cool CD, Newell JD, et al. Lung diseases in patients with common variable immunodeficiency: Chest radiographic, and computed tomographic findings. *J Comput Assist Tomogr* (2006) 30:828–38. doi: 10.1097/01.rct.0000228163.08968.26
- Bondioni MP, Duse M, Plebani A, Soresina A, Notarangelo LD, Berlucchi M, et al. Pulmonary and sinus changes in 45 patients with primary immunodeficiencies: Computed tomography evaluation. *J Comput Assist Tomogr* (2007) 31:620–8. doi: 10.1097/RCT.0b013e31802e3c11
- Manolescu D, Davidescu L, Traila D, Oancea C, Tudorache V. The reliability of lung ultrasound in assessment of idiopathic pulmonary fibrosis. *Clin Interv Aging* (2018) 13:437–49. doi: 10.2147/CIA.S156615
- Wall LA, Wisner EL, Gipson KS, Sorensen RU. Bronchiectasis in primary antibody deficiencies: A multidisciplinary approach. *Front Immunol* (2020) 11:522. doi: 10.3389/fimmu.2020.00522